Residual Stress Measurements of High Spatial Resolution

D. Vogel*, F. Luczak**, B. Michel*

*Fraunhofer IZM, Micro Materials Center, Volmerstrasse 9b, 12489 Berlin, Germany
dietmar.vogel@izm.fraunhofer.de
**Berliner Nanotest und Design GmbH, Volmerstrasse 7b, D-12489 Berlin, Germany
info@nanotest.org

ABSTRACT

Residual stresses in semiconductor and MEMS devices superposing functional and environmental loading are one of the crucial reliability issues. Most of routinely used stress measurement methods today allow stress measurements with only limited spatial resolution. The authors present two approaches under development, which are aiming at stress measurements on micro- and nanoscale devices with proven spatial resolution. The first method bases on stress release due to local material removal by a focused ion beam. SEM images before and after ion milling captured in a FIB equipment are compared to each other by cross correlation algorithms. As a result, residual stresses are evaluated from measured stress relief deformation. The second method refers to EBSD techniques. Displacements of Kikuchi diffraction patterns within a mono-crystalline material area are used to map incremental values of residual stress. Application capability of both stress measurement methods are demonstrated by experiments examples.

Keywords: residual stress, MEMS, semiconductor, stress relief, EBSD

1 INTRODUCTION

Development of new semiconductor and MEMS devices gives rise to several reliability issues to be analyzed and solved. Among them mechanical stresses between and in structural components covering some dimensional magnitudes are one of the concerns. They appear as residual stresses resulting from a multitude of different component processing steps manufacturing micro and nano components.

Unfortunately, stress determination in MEMS/NEMS, semiconductor devices and their packaging is everything else as a simple task. Finite element simulations should include modeling of complete production steps, having impact on final stress profiles. Realistically, this approach cannot be realized for complex devices. Experimentally, the choice of available stress measurement methods with micro- or even nanoscopic spatial resolution is rather limited. The authors developed a new promising stress measurement technique allowing access to stresses in microscopic and nanoscopic system areas. This method bases on the specific testing feasibilities provided by focused ion beam (FIB) equipment. Ion milling is utilized to release very locally residual stresses on components of interest. Generated this way surface deformations around the milled area are measured by digital image correlation (DIC) algorithms. As a result originally existing residual stresses are computed from measured stress release deformations. After a brief introduction to local stress measurement methods this method is described in more detail in chapter 3.

However, measurement of residual stresses with high spatial resolution keeps being a difficult task and is until now a topic under investigation and development. Because of the quite different capabilities of tackled approaches comparison and application of more than one method to a particular problem seems to be desirable. In that sense the authors try to set up different techniques to be combined with each other. A second tool reported here, applies the measurement of slight changes in electron diffraction pattern due to lattice stresses. The application of the method to thin stressed layers is illustrated in chapter 4.

2 LOCAL STRESS MEASUREMENT METHODS

Most available today measurement methods for residual stresses suffer from the fact that they average over larger object areas and cannot be applied very locally, i.e. within areas of a micron or of even substantially smaller size. This is the case for standard equipment used to measure wafer or die bow and conclude from curvatures on thin layer stresses [1]. Only a couple of known tools really allow very local measurement, for instance CBED [2,3], EBSD based approaches [4,5] and microRaman [3] stress techniques. Currently effort is made to extend their scope of measurement towards nanoscopically sized object. Nevertheless these methods also possess specific restrictions for application, in the case of microRaman, e.g., only a limited group of materials of interest can be accessed, which provide suitable Raman lines for Raman shift measurements. However, Raman technique currently is under development to extend spatial measurement resolution significantly beyond the limits of diffraction limited optical resolution, i.e. to address areas of less than 100 nm lateral size [6,7]. EBSD stress investigations demand a reference stress state as incremental strain and stress values can be determined only. Advantageous with

NSTI-Nanotech 2008, www.nsti.org, ISBN 978-1-4200-8503-7 Vol. 1

respect to EBSD measurements is that different elements of the strain / stress tensor can be derived in a direct way and independently from each other.

The developed stress release method of the authors [8-10] intends to meet the goal of high spatial resolution, at the same time considering the method suitable for a larger variety of materials. This technique concludes from the stress release deformation field on stress states utilizing a priori knowledge of the kind of stress field. Analytical derivation or finite element simulation is used to describe stress relaxation due to ion milling and to determine stresses quantitatively by the amount of stress relief displacements. If uncertain, implemented stress hypotheses have to be examined by experimental modifications of stress relief pattern in order to make sure that the right theoretical treatment of the mechanical problem is applied. Stress measurements with the stress release methods, established by the authors as the fibDAC technique, are described in more detail in the following section.

3 STRESS RELIEF TECHNIQUE

3.1 Theory

In contrast to the classical hole drilling method [11] stress relief in semiconductor or MEMS structures, e.g. in thin layers on substrates, is produced by trench milling. Commonly, this choice is made for two reasons. Firstly, trench type geometry provides higher sensitivity with respect to stresses under measurement. Because stress relaxation at milling patterns on thin layers around 100 nm thickness is in the scope of some nanometers even for higher stresses, application of most efficient stress relief structures is necessary. Secondly, trench milling causes a distinguished stress sensitivity in the direction perpendicular to the trench. With some simplifications, the mentioned kind of mechanical problem can be described by an elastic plane strain approach, and was published in [12].

Following [12], the displacements generated when a surface trench is milled into a thin layer are normal to the trench plane and dependent on trench depth, the total film thickness and the ratio of the Young's modulus of the film to that of the substrate. The analytical solution bases on the assumption that the trench is infinitely long and narrow compared with its depth. The trench extends not further than the first interface between the thin film and the substrate. The displacement component perpendicular to the trench direction equals [13]

$$u_x = \frac{2.243}{E'_f}\sigma_o \int_0^a f_1^2 \cdot f_2 \, da \tag{1}$$

Introducing an angle θ, defined by

$$\theta = arctg\left(\frac{x}{a}\right) \tag{2}$$

the integrated functions f_1 and f_2 can be written as

$$f_1\left(\frac{a}{h}\right) = \left(1-\frac{a}{h}\right)^{1/2-S}\left(1+\lambda\frac{a}{h}\right)$$
$$f_2(\theta) = \cos\theta\left(1+\frac{\sin^2\theta}{2(1-\nu_f)}\right)* \tag{3}$$
$$*\left(1.12+0.18\sec h(\tan\theta)\right)$$

x is the independent coordinate perpendicular to the trench, a is the trench depth, h is the thin film thickness. E'_f accounts for the plane strain Young's modulus $E'_f = E_f \big/ (1-\nu_f^2)$ of the film, ν_f for the Poisson ratio and σ_0 for the residual stress. Elastic mismatch between substrate and thin film is taken into account in $f_1(a/h)$ through parameters S and λ. Both of them are related to Dundur's parameters α, β that measure the mismatch in the plane tensile modulus across the interface and in the in-plane bulk modulus, respectively. The parameter S can take values between 0 and 1, being 0.5 in the absence of elastic mismatch, whereas λ is typically small in magnitude and equal to zero in the case of identical film and substrate materials. A detailed description of the matter can be found in [14]. A common way of stress extraction using formulas (1) to (2) is given in the next section.

Besides the analytical solution depicted above, the stress release fields can be computed more accurately by finite element simulations. The numerically obtained x-displacement field is compared to the experimental data. A best fit procedure incorporating a stress scaling factor allows to get the elastically stored residual stress released by ion milling.

3.2 Measurement Example

In order to illustrate capabilities of the stress release method based on solution (1) to (3), a measurement example of a 350 nm thick low pressure chemical vapor deposited (LPCVD) silicon nitride film is given below. The deposition was performed onto a 300 µm thick silicon substrate at 800 ºC under a residual pressure in the range of 190-210 mTorr.

SEM images before and after ion milling were taken at a magnification of approximately 40,000. Under these circumstances accuracy of every single measurement point of displacements equals approximately 0.3 nm. The monitored region was placed at the center of the trench. A displacement field with the displacement component perpendicular to the trench plane has been obtained. As expected, the layer under tensile residual stress experienced an opening under stress release. Fig. 1 shows that the slot depth is asymmetrical; depths of 212 and 272 nm have been milled at left and right sides of the trench, respectively.

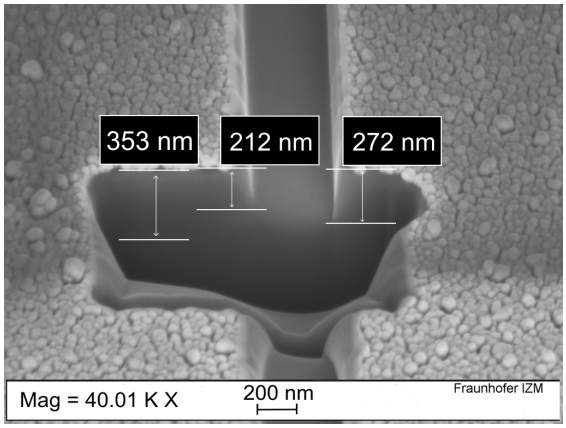

Figure 1: Cross-section of a milled trench in the Si_3N_4 layer on top of the Si substrate

For stress evaluation from the displacement field formulas (1) to (3) have been applied. An approach similar to that described in [12] has been used to extract the isotropic in-plane stress. To make the analysis easier and to improve accuracy, displacement field data points have been averaged along the trench direction. I.e., an average of all displacements at the same distance from the slot has been computed. This implies that all data points within the measurement window on the specimen are assumed to originate from the middle of the trench. The slow drop down of displacements along the trench length justifies this approach. First, a theoretical displacement curve u_x^{ref} is computed from (1) by introducing experimental parameters (i.e. material properties, trench depth and thin film thickness) in the analytical expression, as well as an arbitrary reference stress value. In this way, the analytical expression yields a reference displacement $u_x^{ref}(x)$ at each distance from the trench. Respective measured and averaged displacement values $u_x^{meas}(x)$ are then plotted versus the computed theoretical values taken for the reference stress. Consequently, the slope of the curve yields the ratio between the real stress of the sample and the one computed as reference. Here, a presumed linear behavior of the mechanical response due to ion milling has been taken into account. The intercept of the linear curve with the abscissa axis accounts for rigid body displacement occurred between image captures (before and after ion milling).

Fig. 2 shows the mentioned plot of reference vs. measured displacements for the sample. Data is fitted for the left as well as for the right side of the trench, independently. The presented procedure is advantageous because of the separate treatment of both left and right side displacement fields. In this way the correct trench depth value can be used for either of the trench sides. So, slight differences in trench depths on both sides of the trench lead not to additional errors of stress evaluation. In this method the amount of absolute displacement and the displacement gradient, moving away from the trench rim, is taken as a measure for the released stress, instead of the trench opening / closing amount.

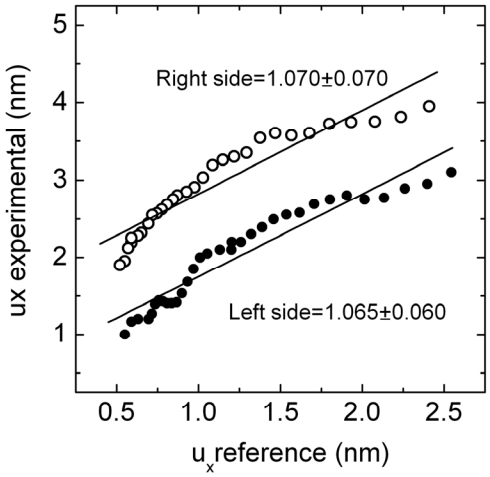

Figure 2: Residual stress determination by trench opening measurement. Fitting of experimental displacement data versus data obtained from the analytical expression (1) at 1 GPa of pre-selected residual stress. Values of the displacement component perpendicular to the trench direction have been averaged over a certain length of the whole trench size.

Material parameters used in the analytical expression of displacements in (1) to (3) and the values of parameters α, β, S and λ have been summarized in Table 1. The Young's modulus of the silicon nitride under study has been obtained from independent nano-indentation measurements.

	Material	
Parameter	silicon	LPCVD Si_3N_4
Young's modulus (GPa)	169 [17]	215 [13]
Poisson ratio	0.27 [17]	0.32 [16]
α	0.120	
β	0.023	
S	0.524	
λ	0.0095	

Table 1: Summary of the material properties and mismatch parameters used in the analytical formulas (1) to (3)

In Fig. 2 the measured displacements $u_x^{meas}(x)$ are plotted against those estimated using the analytical expression $u_x^{ref}(x)$ and assuming a reference tensile stress value of 1 GPa for the right and the left side of the trench, respectively. Stress extraction results obtained on the right and left sides of the trench agree quite well and despite the relatively high data dispersion (R^2 yields a value of 0.89 and 0.91 for left and right side of the trench, respectively). Consequently, the stress value of the layer is determined within an accuracy of 6%. Average stress between both sides yields a value of 1070 ± 70 MPa, which is in very

NSTI-Nanotech 2008, www.nsti.org, ISBN 978-1-4200-8503-7 Vol. 1

good agreement (4%) with a value obtained from the wafer bending test.

4 EBSD BASED STRESS MEASUREMENT

The presented above fibDAC stress relief method is a versatile tool, largely independent on the kind of material to be investigated. However, some restrictions are set by the need of an appropriate residual stress model in order to connect stress relief with stress state. Another method measuring directly crystal lattice deformations relies on tracking of electron back scattered diffraction (EBSD) pattern. It doesn't exhibit the mentioned disadvantage and generally allows stress field measurements with high spatial resolution. Some first test measurements with a commercially available equipment carried out on stressed silicon are reported in the following.

The method makes use of the slight movements of Kikuchi diffraction patterns captured by an EBSD detector [4, 5], which occurs if crystal lattices are deformed by internal stresses. As a result of normal and shear strains as well as crystal rotations, positions of zone axes displace on the phosphorus screen. Combining at least four spatially separated measurements of zone axes displacements within one Kikuchi pattern allows to calculate the deformation tensor values $\frac{\partial u_i}{\partial x_j}(i \neq j)$ and $\frac{\partial u_i}{\partial x_i} - \frac{\partial u_j}{\partial x_j}(i \neq j)$. If the elastic crystal constants are known, all strain and stress tensor components $\varepsilon_{i,j}$ and $\sigma_{i,j}$ can be computed as well. Measurement values are spatially incremental data, i.e strains and stresses have to be adjusted to a known reference state.

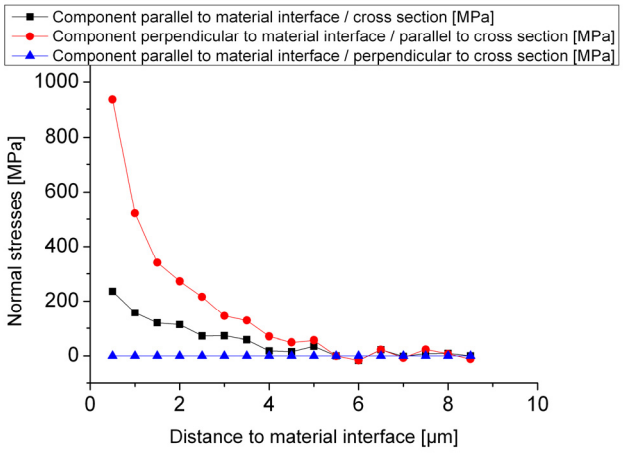

Figure 3: EBSD based stress measurement on Si (stressed by a Si_3N_4 layer), measurement direction perpendicular to layer/substrate interface, $\sigma_{33} = 0$ by definition

Fig. 3 shows measured stresses on a cross sectioned specimen of Si with a highly stressed Si_3N_4 layer on top. It has to be mentioned, that a severe stress re-distribution takes place at the free surface of the cross section. So far measured stresses are not the same as in the inner part, far from the surface. The inner stresses can be computed with the help of finite element simulations on base of the measurement data.

5 CONCLUSIONS

Two advanced methods of very local stress measurement on MEMS and semiconductor structures have been presented. The first technique uses stress relief deformations generated by trench milling with a focused ion beam equipment. Stresses are determined by trench opening / closing displacements. The second technique bases on the analysis of displacements of local EBSD Kikuchi pattern. The first tool allows measurement for a wide range of materials. The latter one is restricted to single crystalline materials, but allows to compute moderate fields of strain and stress tensor components.

REFERENCES

[1] L.B. Freund, S. Suresh, "Thin Film Materials", Cambridge University Press, 2003.

[2] J.A. Nucci, R.R. Keller, St. Kraemer, C.A. Volkert, M.E. Gross, Proc. of Mat. Res. Soc. Symp., Vol. 612, D8.5.1 –D8.5.6.

[3] V. Senez, A. Armigliato, I. de Wolf, G. Carnevale, R. Balboni, S. Frabboni and A. Benedetti, J. Appl. Phys., 94, 5574, 2003.

[4] A.J. Wilkinson, Ultramicroscopy, 62, 237-247, 1996.

[5] A.J. Wilkinson, G. Meaden, D.J. Dingley, Ultramicroscopy, 106, 307-313, 2006.

[6] .C. Georgi, M. Hecker, E. Zschech, Appl. Phys. Letters, 90, 171102, 2007.

[7] R. Ossikovski, Qu. Nguyen, G. Picardi, Physical Review, B 75, 1, 2007.

[8] D. Vogel, et al., Proc. of SPIE, Vol. 5766 (2005).

[9] N. Sabaté, D. Vogel, A. Gollhardt, J. Keller, B. Michel, C. Cané, I. Gràcia, J. R. Morante, Appl. Physics Letters 88, 071910, 2006

[10] D. Vogel, A. Gollhardt, N. Sabate, J. Keller, B. Michel, H. Reichl, Proc. of ECTC 2007, Reno 1490-1497, 2007.

[11] ASTM Standard "Test Method for Determining Residual Stresses by the Hole-Drilling Strain-Gage Method", E837-01e1, 2001.

[12] Ki-Ju Kang, et al, Journal of Engineering Materials and Technology, 126, October, 457-464, (2004).

[13] J.W. Hutchinson, Z. Suo, Advances in Applied Mechanics, 29, 63-191, 1992.

[14] J. Dundurs, D.B. Bogy, Journal of Applied Mechanics, 36, No. 3, 650, 1969.